



Design and development of anisotropic inorganic/polystyrene nanocomposites by surface modification of zinc oxide nanoparticles



Xiao Han^{a,b}, Shiming Huang^c, Yilong Wang^{b,*}, Donglu Shi^{b,d,**}

^a School of Materials Science and Engineering, Tongji University, Shanghai 200092, PR China

^b Research Center for Translational Medicine, East Hospital, the Institute for Biomedical Engineering & Nano Science, Tongji University School of Medicine, Shanghai 200092, PR China

^c Department of Physics, Tongji University, Shanghai 200092, PR China

^d The Materials Science and Engineering Program, College of Engineering and Applied Science, University of Cincinnati, Cincinnati, OH 45221, USA

ARTICLE INFO

Article history:

Received 16 December 2015

Received in revised form 11 February 2016

Accepted 19 March 2016

Available online 22 March 2016

Keywords:

Anisotropic nanocomposites

Surface modified zinc oxide

Oleic acid

Miniemulsion polymerization

ABSTRACT

Anisotropic yolk/shell or Janus inorganic/polystyrene nanocomposites were prepared by combining miniemulsion polymerization and sol–gel reaction. The morphologies of the anisotropic composites were found to be greatly influenced by surface modification of zinc oxide (ZnO) nanoparticle seeds. Two different types of the oleic acid modified ZnO nanoparticles (OA-ZnO) were prepared by post-treatment of commercial ZnO powder and homemade OA-ZnO nanoparticles. The morphologies and properties of the nanocomposites were investigated by transmission electron microscope (TEM), thermogravimetric analysis (TGA), Fourier transform infrared spectroscopy (FT-IR), dynamic light scattering (DLS), and energy dispersive X-ray spectroscopy (EDX). It was found that both post-treated OA-ZnO and in-situ prepared OA-ZnO nanoparticles resulted in the yolk–shell and Janus structure nanocomposites, but with varied size and morphology. These nanocomposites showed stable and strong fluorescence by introducing quantum dots as the co-seeds. The fluorescent anisotropic nanocomposites were decorated separately with surface carboxyl and hydroxyl groups. These composites with unique anisotropic properties will have high potential in biomedical applications, particularly in bio-detection.

© 2016 Elsevier B.V. All rights reserved.

1. Introduction

The concept of “Janus particles”, which named after the two-faced Roman God Janus, was first raised by P. G. de Gennes in his Nobel Prize address in 1991 [1]. “Janus” particles are asymmetric and anisotropic in structure, shape, and surface characteristics with each surface having distinctively different physical and chemical properties [2]. Due to the unique geometrical asymmetry, Janus nanoparticles can be used as ideal drug delivery carriers, catalysis, surfactants, and biosensor [3–5]. Several strategies have been developed to synthesize asymmetrical nanoparticles. These include the layer-by-layer self-assembly [6,7], evaporated metal particles [8–11], Pickering emulsion method [12], biphasic electrified jetting [13,14], photo-polymerization in a microfluidic channel [15,16], and polymer self-assembly [17,18]. Janus particles can assume different geometries: spherical, dumbbell, half raspberry-like, cylindrical, disk, and a variety of other shapes [2]. Besides Janus composites, yolk–shell like nanocomposites was also a newly emerging system for biomedical applications [19,20]. The functional core and hollow shell

of the yolk–shell particles can be tailored to the requirements of the nanoreactors [21] and biomedicine [22]. The common and typical synthesis of the yolk/shell particles includes the following, namely, selective etching or dissolution, bottom-up or soft-template, ship-in-bottle, Ostwald ripening or galvanic replacement process, and Kirkendall diffusion methods [22]. The Janus or yolk–shell nanoparticles are usually composed of inorganic–inorganic dimmer or inorganic–polymer composites [23–26]. Among these, the silica/polystyrene composites is one of the most frequently studied systems [27,28] and the silica/magnetite/polymer composites have been developed into the ternary system [29–31]. The straightforwardness and yield of the reaction have been important factors in the development of the synthetic methods. We have previously reported a one-step facile method based on oleic acid modified iron oxide nanoparticles via combined miniemulsion polymerization and sol–gel reaction for preparing the ternary magnetic composites with Janus or yolk–shell morphologies [32,33]. Such magnetic nanomaterials have demonstrated some advantages in bio-detection of rare target by magnetic collection utilizing the active surface functionality. However, the role of the oleic acid modified inorganic nanoparticles was not well understood in the formation of the ternary composites. Few literatures have been reported about the bilateral system, particularly on the influence of the surface chemistry of Titania hydrosols on the stability and morphology of the hybrid nanoparticles [34].

* Corresponding author at: Mailbox 155#, Siping Road 1239, Yangpu District, Shanghai, 200092, PR China.

** Correspondence to: D. Shi, Research Center for Translational Medicine, East Hospital, the Institute for Biomedical Engineering & Nano Science, Tongji University School of Medicine, Shanghai 200092, PR China.

E-mail addresses: yilongwang@tongji.edu.cn (Y. Wang), shid@ucmail.uc.edu (D. Shi).

In this study, we investigated the effect of surface modification of the oleic acid modified zinc oxide (OA-ZnO) nanoparticles on the composite size and morphologies using a one-pot synthesis process. Two different particle systems were investigated: the OA-ZnO nanoparticles were developed in an in-situ synthesis with simultaneous surface modification, and the other by post-modification of commercialized zinc oxide powder. The oleic acid modified zinc oxide was used as the inorganic seeds. Polystyrene/ZnO@SiO₂ nanocomposites were prepared via a combined process of miniemulsion polymerization and sol-gel reaction. For bio-detection applications, carboxyl group was introduced to the surface of the polymer component for conjugation of antibody. The ternary system without magnetic component was further developed into a fluorescent probe by conjugating with the hydrophobic quantum dots for immune detection of biomarkers via a sandwich method.

2. Materials and experiments

2.1. Materials

All reagents used were analytical grade and available commercially. Zinc oxide (ZnO) was purchased from Emperor Nano Material Co. (Nanjing, China). Oleic acid (OA, 90%) was purchased from Shanghai Chemical Reagents Co. (Shanghai, China). Styrene (St), ammonium hydroxide (NH₄OH, 28 wt %), and Sodium hydroxide (NaOH) were purchased from Sinopharm Chemical Reagent Co. (Shanghai, China). Tetraethoxysilane (TEOS), sodium dodecyl sulfate (SDS) and 4, 4'-Azobis (4-cyanovaleic acid) (ACVA) were purchased from Sigma-Aldrich (USA). Hexadecane (HD) was purchased from Acros Organics (USA). Hydrophobic quantum dots (CdSSe/ZnS core shell nanocrystals with particle size of 9 nm and molecular weight of 7.5×10^5) were purchased from Nanjing technology Co. (Hangzhou, China).

The aforementioned chemicals were used as received. Styrene was washed first with 5 wt % sodium hydroxide solution and stored at -20°C before using. High-purity nitrogen gas, provided by a local supplier, was used for sparging solutions without further purification. Deionized (DI) water was used throughout the entire experiment.

2.2. Synthesis of oleic acid-modified zinc oxide nanoparticles

OA-ZnO-a nanoparticles were fabricated by surface modification of the commercial ZnO powder. With the index of particles' size by Dynamic Laser Scattering (DLS) measurement, the orthogonal experiments were carried out to optimize liquid–solid ratio, mixing time, and the reaction temperature and time for surface modification of the commercial ZnO powder. The optimum modification condition was determined as follows. Briefly, oleic acid (1.94 mL) was dissolved in ethanol (50 mL) with mechanical stirring. After adding ZnO nanoparticles (0.25 g), the dispersion was heated to 60°C which under 200 W sonication (KQ-400KDV, Kunshan Ultrasonic Instruments Co, Ltd.) for 3 h. Finally, the dispersion was cooled down to room temperature.

Another type of OA-ZnO nanoparticles (OA-ZnO-b) was synthesized via a modified process according to Heyon's work [35]. Both types of OA-ZnO nanoparticles were collected by a centrifugal machine (3000 rpm/min, 10 min), and the precipitate was dispersed in 50 mL ethanol and DI water with ultrasonication for 10 min. The washing procedure was repeated for five times and the precipitate was dried by freezing-drying for further use. The extra oleate and oleic acid was removed from both OA-ZnO-a and OA-ZnO-b nanoparticles by washing.

2.3. Synthesis of polystyrene/ZnO@SiO₂ nanocomposites

Anisotropic polystyrene/ZnO@SiO₂ nanocomposites were prepared via a combined process of miniemulsion polymerization and sol-gel reaction reported by our group [32]. The water phase was prepared by dissolving 0.092 g SDS in 39 g of DI water. The oil phase was prepared

by the following steps: HD (0.4 g) was first dissolved in St monomer (7 g) by 3 min sonication, then OA-ZnO nanoparticles powder (0.025 g) was then dissolved in the monomer phase. TEOS (2 g) was subsequently resolved into the mixture of the hydrophobic components. The water phase and oil phase were mixed by dropping the oil dispersion dropwise to the water phase under 200 W sonication (KQ-400KDV, Kun Shan Ultrasonic Instruments Co., Ltd., China), followed by 250 rpm mechanical stirring for 30 min. Miniemulsion droplets system was developed by sonicating the emulsions at 500 W in an ice bath with a duty cycle of 50% for 20 min by a Scientz-IID sonifier (JY92-2D, Ningbo Xinzhi Bio-technology Co., Ltd., China). Upon neutralizing 0.12 g of ACVA by 1 mL of NaOH solution (0.856 M) and added into the flask, the system was deoxygenized by nitrogen bubbling for 0.5 h with 250 rpm mechanical stirring. With a condenser under nitrogen protection, the flask was moved into 70°C water bath to initiate St monomer polymerization. After reaction for 1.5 h, 50 μL of NH₄OH was added into the reaction. After heating for another 5 h, the reaction system was stirred at room temperature overnight. The final polystyrene/ZnO@SiO₂ nanocomposites were obtained by centrifugal separation.

2.4. Synthesis of QDs@ polystyrene/ZnO@SiO₂ nanocomposites

The fluorescent nanocomposites were developed by doping a controlled amount of hydrophobic QDs (5 mg) with the OA-ZnO nanoparticles into the oil phase. The steps were kept the same as synthesis of polystyrene/ZnO@SiO₂ nanocomposites.

2.5. Characterization

Transmission electron microscopy (TEM). The washed composite particles were dispersed in DI water and dried onto carbon-coated copper grids before examination. TEM images and energy dispersive X-ray (EDX) analysis were obtained with a Philips Tecnai 20 electron microscope.

Thermogravimetric analysis (TGA). A thermogravimetric analyzer (Netzsch TG209, Germany) was used to analyze the surface modification of the OA-ZnO. The measurement was performed under a nitrogen atmosphere from ambient temperature to 900°C with a heating rate of $10^\circ\text{C}/\text{min}$.

Fourier transform infrared spectroscopy (FT-IR). FT-IR spectra of unmodified ZnO and the OA-ZnO nanoparticles were obtained by using the infrared spectrometer (Bruker Tensor 27, USA).

Dynamic light scattering (DLS). Hydrodynamic size of the nanocomposites and purified OA-ZnO nanoparticles were measured by the DLS instrument (Zetasizer Nano-ZS, Malvern, U.K.).

Fluorescence spectra. The fluorescence of QDs and composite nanoparticles were measured using a spectrophotometer (LS-55, Perkin-Elmer, USA) at room temperature. Fluorescent composites were dropped on glass slide.

Fluorescent imaging system. After dropping the fluorescent sample onto a glass slide, the fluorescence imaging was performed by using an inverted fluorescence microscope (Nikon ECLIPSE Ti, Japan).

3. Results and discussion

Fig. 1 shows the TEM images and DLS data of OA-ZnO-a and OA-ZnO-b. As shown in Fig. 1A, OA-ZnO-a is of irregular shape with an average size of 25 nm. In Fig. 1B, OA-ZnO-b mainly consists of mono-dispersed spherical particles of a size about 15 nm. Note that in the former (OA-ZnO-a), the oleic acid was functionalized by post-treatment of the commercial ZnO powder and in the latter (OA-ZnO-b), the nanocrystals were surface-functionalized during the in-situ synthesis. With oleic acid coating, DLS data of the two kinds of OA-ZnO nanoparticles show good dispersion in the organic solvent. Upon surface modification, the hydrophobicity of the commercial ZnO particle was dramatically improved. The hydrodynamic average diameter of OA-ZnO-a (Fig. 1C) is

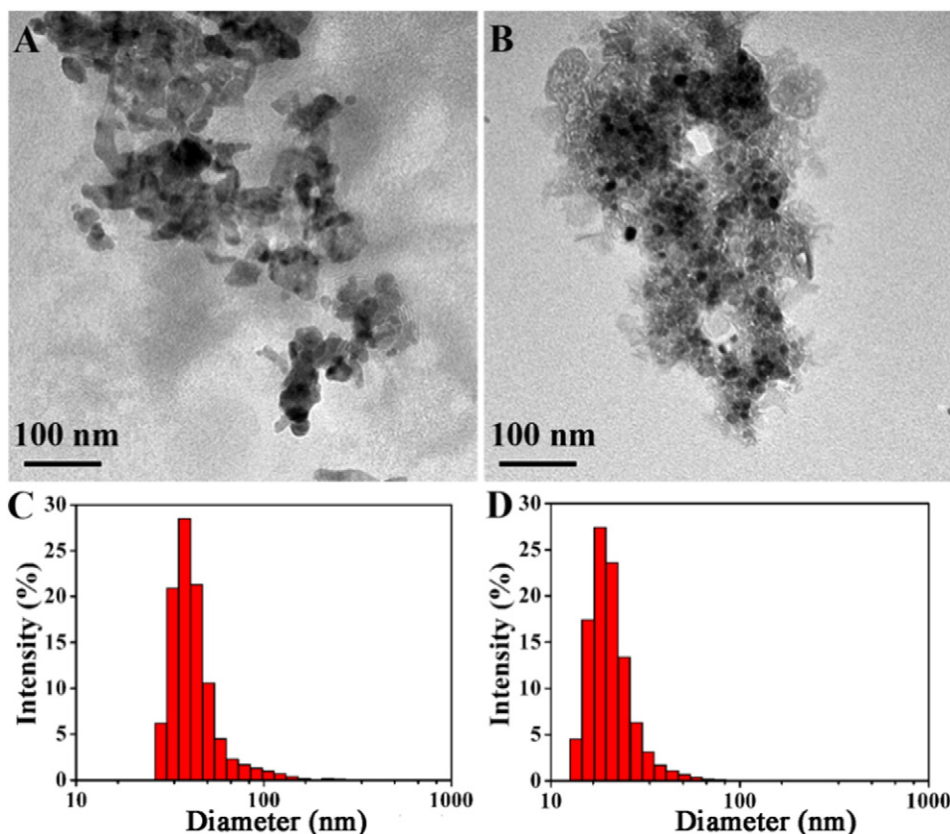


Fig. 1. TEM images and DLS data of two kinds of oleic acid modified zinc oxide nanoparticles: OA-ZnO-a (A, C) and OA-ZnO-b (B, D).

close to 37 nm (Poly-dispersity Index, PDI: 0.315), indicating well functionalized ZnO particles in this process. The DLS diameter of OA-ZnO-b (Fig. 1D) is about 20 nm (PDI: 0.323), which is consistent with TEM results.

The surface modification of the ZnO particles was further characterized by FT-IR and TGA. Fig. 2A shows the FT-IR absorption spectra of oleic acid (OA), OA-ZnO-a and OA-ZnO-b. As can be seen in Fig. 2A, there are strong vibrations bands of $-\text{CH}_3$ and $-\text{CH}_2$ groups from both OA-ZnO at 2850 and 2920 cm^{-1} , indicating the nanoparticles' surface oleic acid molecules. However, peaks at $1725\text{--}1700\text{ cm}^{-1}$ due to the stretching vibrations of $\text{C}=\text{O}$ group in free oleic acid are not observed in the spectra of OA-ZnO-a and OA-ZnO-b. Furthermore, the peaks at 1544 cm^{-1} are attributed to the stretching vibrations of $\text{COO}-\text{Zn}$, due to the interaction between the $-\text{COOH}$ group of the oleic acid and the $-\text{OH}$ group on the surface of ZnO nanoparticles [36–38]. These results show chemically well grafted surfaces of the ZnO nanoparticles.

Fig. 2B shows the thermogravimetric (TGA) curves of the original commercial ZnO powder, OA-ZnO-a, and OA-ZnO-b. The mass of unmodified ZnO powders was found almost unchanged after the heating process. The weight loss of OA-ZnO-a in the temperature range of $150\text{--}700\text{ }^\circ\text{C}$ was 47.0 wt %, due to thermal decomposition of the multi-layer oleate. Only 11 wt % weight loss of OA-ZnO-b nanoparticles, in the range of $150\text{--}700\text{ }^\circ\text{C}$, was detected resulting from the decomposition of oleate. Due to excess oleic acid in ZnO-a, excessive OA molecules are adsorbed on the first OA layer in the form of end-end hydrophobic interaction [39]. The primary layer is presumed to chemically adsorb on the surfaces of the nanoparticles. The irregular shape of the commercial ZnO nanoparticles may occupy more oleic acid molecules.

Fig. 3A and B shows the TEM micrographs of the typical composites obtained from the two types ZnO nanoparticles. The composites exhibit the cell-like yolk-shell structures composed of the polystyrene core and inorganic shell with the OA-ZnO-a seeds. As shown in Fig. 3, only a small

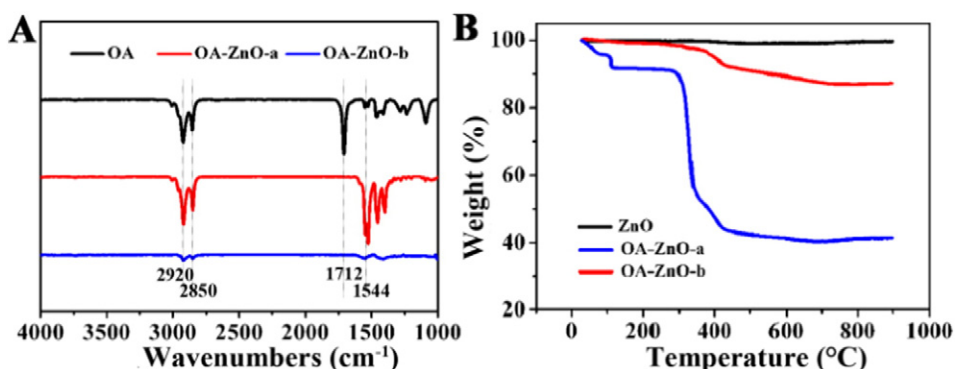


Fig. 2. FT-IR spectra and TGA analysis curves of the modified ZnO nanoparticles.

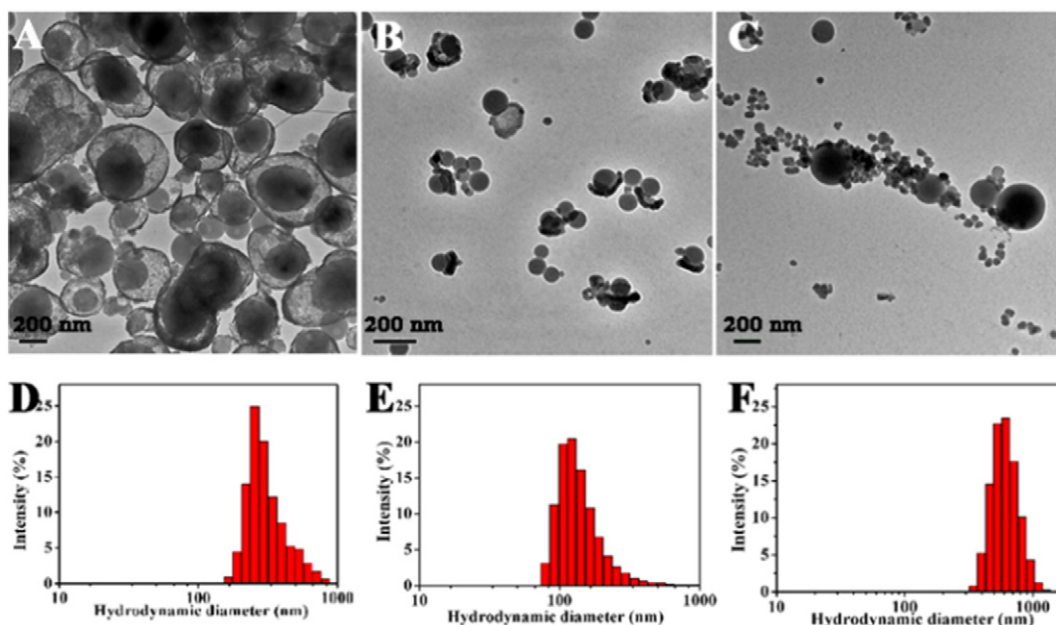


Fig. 3. TEM images and DLS data of ZnO/silica/polystyrene composites obtained when: (A, D) OA-ZnO-a as the seeds, (B, E) OA-ZnO-b as the seeds, and (C, F) without ZnO seeds.

fraction displays the regular spherical shape, while the rest is ellipsoid. The average size of the composites and the polystyrene cores are 550 and 370 nm, respectively. There is a clear space between the core and shell. Using OA-ZnO-b as the seeds, the product is Janus-like nanocomposites. The structure is similar to the Fe₃O₄@silica/polystyrene ternary composites reported in our previous work [32]. Even under the same polymerizing conditions, the morphologies of the two types of composites (i.e. OA-ZnO-a and OA-ZnO-b) are entirely different. The difference in morphology is attributable to their surface properties resulting from the diverse oleic acid modification methods. Emulsification procedure involving a fusion/fission process during the mechanical stirring and sonication is necessary before polymerization in the miniemulsion system [40]. The monolayer or multilayer of OA on ZnO will have a strong effect on dispersion and morphology of the nanoparticles in the miniemulsion droplets [41]. The Janus composites based on OA-ZnO-b have the 100 nm PS cores as shown in Fig. 3B, and half-arc silica shell with the thickness of around 30 nm. Fig. 3D shows, based on the DLS data, an average size of 390 nm for the yolk-shell composites with a polydispersity index of 0.385, and 140 nm for Janus composites with a polydispersity index of 0.314. The differences in morphology and size indicate an important factor of using different inorganic seeds. To investigate the role of the OA-ZnO nanoparticles in the reaction, we performed the miniemulsion polymerization in the absence of any modified ZnO nanoparticles under the same processing condition. As a result, as shown in Fig. 3C, neither Janus nor yolk-shell structures is obtained. Only separated large polystyrene latexes and small silica particles are observed with hydrodynamic diameter about 600 nm. This result of control experiment shows the direct effect of the inorganic seeds on the final composite structures.

The nucleation of miniemulsion polymerization is distinctly different with conventional emulsion polymerization which takes place in the monomer droplets. When the solubility of the hydrophobe (i.e. co-stabilizer) in water increases, the rate of Ostwald ripening is increased [42]. These oleic acid modified inorganic particles may act as the co-stabilizer to engender the miniemulsification process [43,44]. Based on the TGA and TEM data result, we found that the size of nanocomposites and polystyrene core was related to the amount of oleic acid grafted on the surface of ZnO nanoparticles.

The composition of the inorganic layer was characterized by TEM-EDX. Fig. 4 shows the EDX spectra of a typical ternary composite particle. As can be seen in Fig. 4, there are elements of silicon and zinc

for each composites, indicating the hybrid composition of the inorganic shell.

Due to the unique structure and properties of yolk-shell and Janus composites, the composites can be conjugated with plenty of QDs as fluorescent probes for cell labeling and tracking. Fig. 5 shows the fluorescence spectra and images of pure QDs and QDs/polystyrene/ZnO@SiO₂ nanocomposites. The emission peak of pure QDs is at 605 nm. The fluorescence spectra of the QDs/yolk-shell composites-a (black line) and QDs/Janus composite-b (blue line) show successful incorporation of QDs into the ternary composite particles. Fig. 5B and C show the fluorescent images of the composites conjugated with QDs. By integrating the fluorescence and other functionalities via surface carboxyl groups, the nanocomposites will have potential applications in bio-detection such as the immune-probes.

Fig. 6 is the schematic diagram showing the synthesis procedure of the composites particles via miniemulsion polymerization and sol-gel reaction. The one-pot miniemulsion process is similar to the method reported in one of our earlier studies. The process can be described as follows: (1) the typical miniemulsify process is developed from water phase and oil phase. Styrene monomer, tetraethoxysilane, hexadecane, and oleic acid-functionalized zinc oxides are restricted in miniemulsion droplets (stage b). (2) Polymerization of St monomers is initiated by initiator 4,4'-Azobis(4-cyanovaleric acid) at 70 °C. As a result of St monomer polymerizing and phase separation, the intermediate product is produced (stage c). (3) After ammonium hydroxide is added, TEOS starts to hydrolyze and poly-condense, simultaneously. The OA-ZnO further separates from the oil phase because the oleic acid molecules will transform to oleate in aqueous alkali. As a result of the lowest systematic energy, the formed silica chains tend to hybridize with zinc oxide particles. The St monomer diffuses inwardly to the PS particles, but TEOS outwardly to the inorganic shell. As the St monomer and TEOS precursors in the droplets are almost exhausted, Janus nanocomposites with a PS core and an ZnO/silica hybrid shell are developed (stage d).

4. Conclusion

In summary, we have employed a one-pot synthesis for preparation of non-magnetic anisotropic nanocomposites. Typically yolk-shell or Janus composites are obtained with two different approaches: post-treatment of commercial ZnO and homemade OA-ZnO seeds.

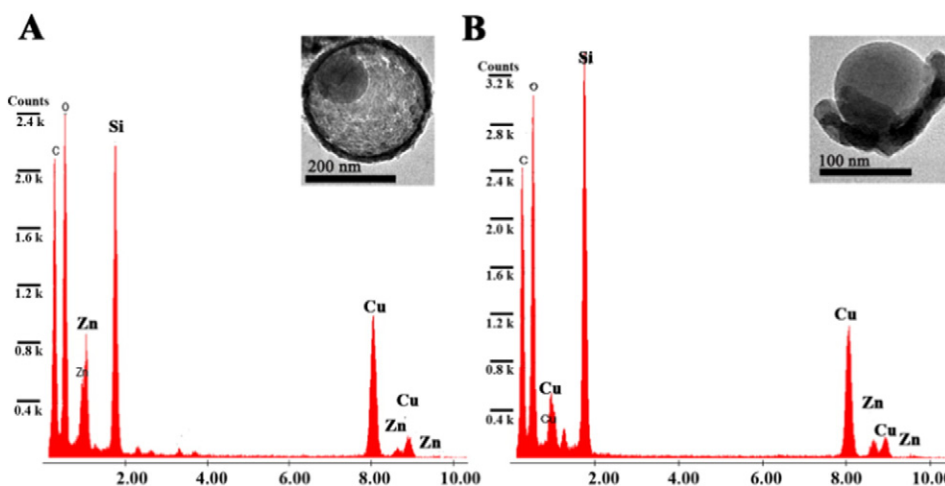


Fig. 4. TEM-EDX spectra obtained from an individual composite particle shown in the inset photos.

These different seeding methods result in varied morphology and size of the final product. The surface modification of the ZnO nanoparticles is found to be the predominant factor. Stable fluorescent composites

have also been synthesized by conjugating the hydrophobic QDs. The anisotropically located carboxyl and hydroxyl groups on asymmetrical single particle surface of the nanocomposites will have unique

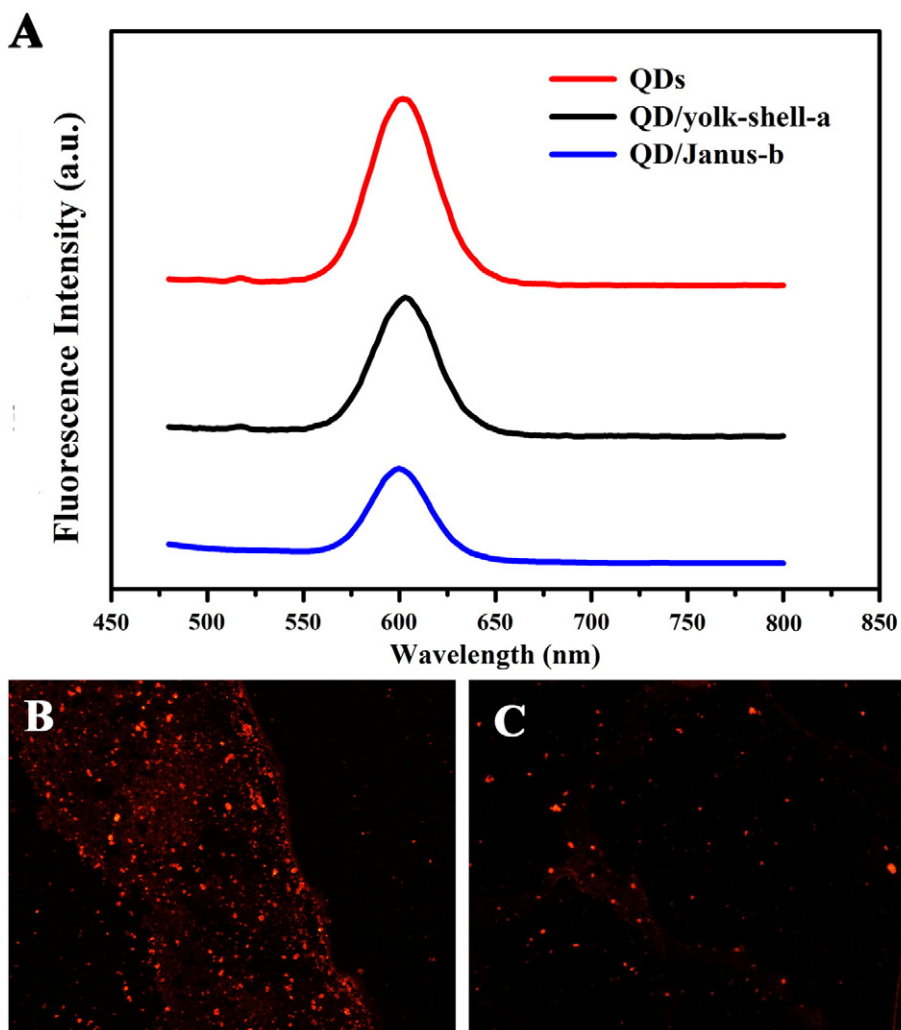


Fig. 5. Fluorescence spectra of pure quantum dots (QDs, red line), QDs/yolk-shell composite – a (black line), and QDs/Janus composite – b (blue line) (A). Fluorescence microscope images of the QDs/yolk-shell composites – a (B) and QDs/Janus composites – b (C).

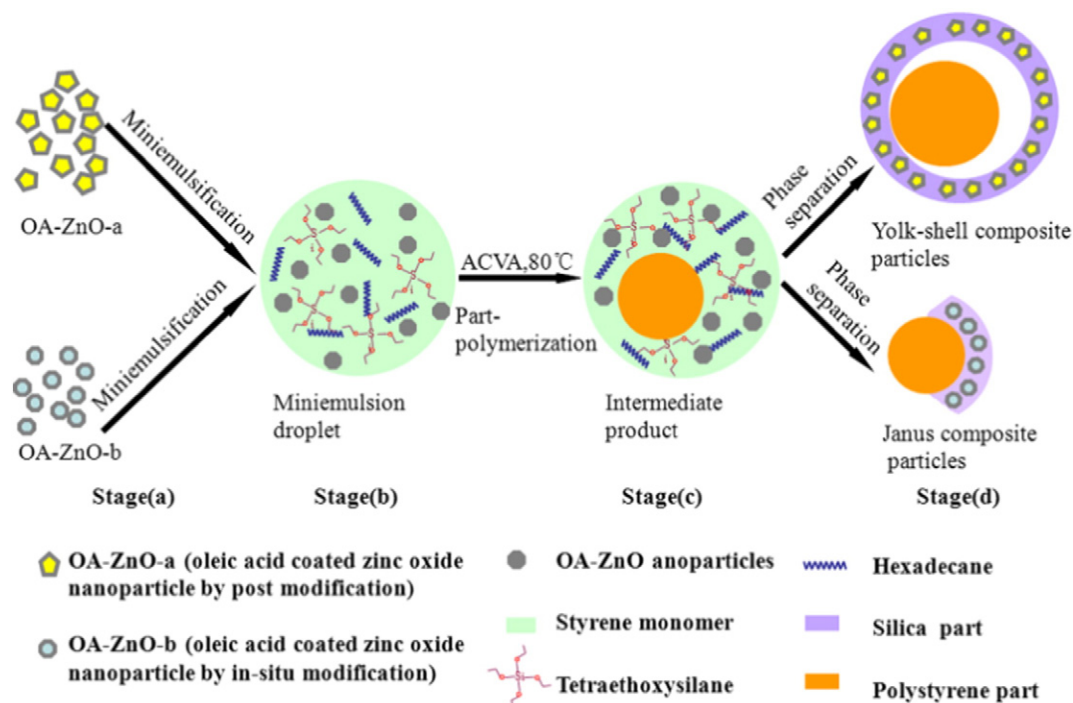


Fig. 6. Schematic illustration shows the pathway for preparation of the nanocomposites via a combined process of miniemulsion polymerization and sol-gel reaction.

applications in biodetection. The fluorescent experimental results elementarily show that non-magnetic anisotropic nanocomposites with good fluorescent performance are ideal carriers for bio-detection applications.

Acknowledgments

This work was supported by the National Natural Science Foundation of China (Nos. 51173135, 31571018), the Science and Technology Commission of Shanghai Municipality (Nos. 15ZR1443200, 15441905900).

References

- [1] P.G. de Gennes, *Rev. Mod. Phys.* 64 (1992) 645–648.
- [2] J. Hu, S. Zhou, Y. Sun, X. Fang, L. Wu, *Chem. Soc. Rev.* 41 (2012) 4356–4378.
- [3] S. Berger, A. Synytska, L. Ionov, K.-J. Eichhorn, M. Stamm, *Macromolecules* 41 (2008) 9669–9676.
- [4] Y.K. Takahara, S. Ikeda, S. Ishino, K. Tachi, K. Ikeue, T. Sakata, T. Hasegawa, H. Mori, M. Matsumura, B. Ohtani, *J. Am. Chem. Soc.* 127 (2005) 6271–6275.
- [5] P. Biji, A. Patnaik, *Analyst* 137 (2012) 4795–4801.
- [6] H.Y. Koo, D.K. Yi, S.J. Yoo, D.Y. Kim, *Adv. Mater.* 16 (2004) 274–277.
- [7] Z.F. Li, D.Y. Lee, M.F. Rubner, R.E. Cohen, *Macromolecules* 38 (2005) 7876–7879.
- [8] J.R. Howse, R.A.L. Jones, A.J. Ryan, T. Gough, R. Vafabakhsh, R. Golestanian, *Physical Review Letters*, 99, 2007.
- [9] H. Takei, N. Shimizu, *Langmuir* 13 (1997) 1865–1868.
- [10] O. Cayre, V.N. Paunov, O.D. Velev, *J. Mater. Chem.* 13 (2003) 2445–2450.
- [11] Y. Lu, H. Xiong, X.C. Jiang, Y.N. Xia, M. Prentiss, G.M. Whitesides, *J. Am. Chem. Soc.* 125 (2003) 12724–12725.
- [12] Y. Wang, B.-H. Guo, X. Wan, J. Xu, X. Wang, Y.-P. Zhang, *Polymer* 50 (2009) 3361–3369.
- [13] K.-H. Roh, M. Yoshida, J. Lahann, *Langmuir* 23 (2007) 5683–5688.
- [14] S. Hwang, K.-H. Roh, D.W. Lim, G. Wang, C. Uher, J. Lahann, *Phys. Chem. Chem. Phys.* 12 (2010) 11894–11899.
- [15] D. Dendukuri, P.S. Doyle, *Adv. Mater.* 21 (2009) 4071–4086.
- [16] R.F. Shepherd, J.C. Conrad, S.K. Rhodes, D.R. Link, M. Marquez, D.A. Weitz, J.A. Lewis, *Langmuir* 22 (2006) 8618–8622.
- [17] R. Erhardt, M.F. Zhang, A. Boker, H. Zettl, C. Abetz, P. Frederik, G. Krausch, V. Abetz, A.H.E. Muller, *J. Am. Chem. Soc.* 125 (2003) 3260–3267.
- [18] I.K. Voets, R. Fokkink, T. Hellweg, S.M. King, P. de Waard, A. de Keizer, M.A.C. Stuart, *Soft Matter* 5 (2009) 999–1005.
- [19] S. Li, J. Zheng, D. Chen, Y. Wu, W. Zhang, F. Zheng, J. Cao, H. Ma, Y. Liu, *Nanoscale* 5 (2013) 11718–11724.
- [20] J. Gao, G. Liang, J.S. Cheung, Y. Pan, Y. Kuang, F. Zhao, B. Zhang, X. Zhang, E.X. Wu, B. Xu, *J. Am. Chem. Soc.* 130 (2008) 11828–11833.
- [21] J. Lee, J.C. Park, H. Song, *Adv. Mater.* 20 (2008) 1523–1528.
- [22] J. Liu, S.Z. Qiao, J.S. Chen, X.W. Lou, X. Xing, G.Q. Lu, *Chem. Commun.* 47 (2011) 12578–12591.
- [23] H.W. Gu, R.K. Zheng, X.X. Zhang, B. Xu, *J. Am. Chem. Soc.* 126 (2004) 5664–5665.
- [24] H. Yu, M. Chen, P.M. Rice, S.X. Wang, R.L. White, S.H. Sun, *Nano Lett.* 5 (2005) 379–382.
- [25] V. Nandwana, G.S. Chaubey, K. Yano, C.-b. Rong, J.P. Liu, *Journal of Applied Physics*, 105, 2009.
- [26] W. Qiang, Y. Wang, P. He, H. Xu, H. Gu, D. Shi, *Langmuir* 24 (2008) 606–608.
- [27] W. Mu, M. Fu, *Microelectron. Eng.* 96 (2012) 51–55.
- [28] Z. Han, L. Wang, J. Zhu, S. Zhang, W. Zhou, *J. Appl. Polym. Sci.* 122 (2011) 43–49.
- [29] M.D. Butterworth, L. Illum, S.S. Davis, *Colloids Surf. A Physicochem. Eng. Asp.* 179 (2001) 93–102.
- [30] M.D. Butterworth, S.A. Bell, S.P. Armes, A.W. Simpson, *J. Colloid Interface Sci.* 183 (1996) 91–99.
- [31] H. Xu, L. Cui, N. Tong, H. Gu, *J. Am. Chem. Soc.* 128 (2006) 15582–15583.
- [32] F. Wang, G.M. Pualetti, J. Wang, J. Zhang, R.C. Ewing, Y. Wang, D. Shi, *Adv. Mater.* 25 (2013) 3485–3489.
- [33] Y. Wang, F. Wang, B. Chen, H. Xu, D. Shi, *Chem. Commun.* 47 (2011) 10350–10352.
- [34] Y. Zhao, H. Wang, X. Song, Q. Du, *Macromol. Chem. Phys.* 211 (2010) 2517–2529.
- [35] S.H. Choi, E.G. Kim, J. Park, K. An, N. Lee, S.C. Kim, T. Hyeon, *J. Phys. Chem. B* 109 (2005) 14792–14794.
- [36] R.Y. Hong, T.T. Pan, J.Z. Qian, H.Z. Li, *Chem. Eng. J.* 119 (2006) 71–81.
- [37] M. Li, B. Hari, X. Lv, X. Ma, F. Sun, L. Tang, Z. Wang, *Mater. Lett.* 61 (2007) 690–693.
- [38] P. Liu, Z.X. Su, *J. Macromol. Sci. Phys. B45* (2006) 131–138.
- [39] L.F. Shen, P.E. Laibinis, T.A. Hatton, *Langmuir* 15 (1999) 447–453.
- [40] M. Antonietti, K. Landfester, *Prog. Polym. Sci.* 27 (2002) 689–757.
- [41] F. Yan, J. Li, J. Zhang, F. Liu, W. Yang, *J. Nanoparticle Res.* 11 (2009) 289–296.
- [42] S. Lu, J. Forcada, *J. Polym. Sci. A Polym. Chem.* 44 (2006) 4187–4203.
- [43] C.S. Chern, T.J. Chen, *Colloids Surf. A Physicochem. Eng. Asp.* 138 (1998) 65–74.
- [44] C.S. Chern, H.T. Chang, *Polym. Int.* 51 (2002) 1428–1438.